

c-IAP1 and UbcH5 promote K11-linked polyubiquitination of RIP1 in TNF signaling

Jasmin N. Dynek, Tatiana Goncharov, Erin C. Dueber, Anna V. Fedorova, Anita Izrael-Tomasevic, Lilian Phu, Elizabeth Helgason, Wayne J. Fairbrother, Kurt Deshayes, Donald S. Kirkpatrick, and Domagoj Vucic

Supplemental Materials and Methods

Yeast two-hybrid constructs

To generate yeast two hybrid bait constructs DNA encoding the c-IAP1, c-IAP2, ML-IAP, XIAP, TRAF2, or TRAF6 RING domains were amplified using the following primers: for c-IAP1, 5'-CAATCATATGGGTCTGTCACTGGAAGAA-3' and 5'-GACTGAATTC CTAAGAGAGAAATGTACGA-3'; for c-IAP2, 5'-CAATCATATGGATCTACCAGTGGGAAGAA-3 and 5'-GACTGAATTCTCATGAAAGAAATGTACG-3'; for ML-IAP, 5'-CAATCATATGGCCAGGGATGTGGAGGCG-3' and 5'-GACTGAATTCTTAGGACAGGAAGGTGCGC-3'; for XIAP, 5'-CAATCATATGGAGATTAGTACTGAAGAG-3' and 5'-GACTGACTCATATGGAGATTAGTACTGAAGAG-3'; for TRAF2, 5'-GATACATATGGGCTTCTCCAAGACCCTC-3' and 5'-CGTAGAATTCCTAGTGAACACAGGCAGCACA-3'; and for TRAF6, 5'-GACGATTGCATATGGAGTTTGACCCACCCCTG-3' and 5'-CTACGAATTCCTACCAGCAGTATTTCAATTGTCAAC-3'. The resultant products were digested with NdeI and EcoRI, and ligated into the pGBKT7 vector (Clontech). The QuikChange site-directed mutagenesis kit (Stratagene) was used to introduce the E2 binding interface (c-IAP1 RING V573A, c-IAP2 RING V559A, ML-IAP RING V254A, and XIAP I452A) and dimerization (c-IAP1 RING F616A, c-IAP2 RING F602A, ML-IAP RING F296A, and XIAP F495A) mutations into the IAP RING domain bait constructs according to the manufacturer's instructions.

To generate yeast two hybrid prey constructs DNA encoding the c-IAP1, c-IAP2, ML-IAP, or XIAP RING domains were amplified using the following primers: for c-IAP1, 5'-GACTGAATTCGTGGTCTGTCACTGGAAGAA-3' and 5'-TCAACTCGAGCTAAGAGAGAAATGTACGA-3'; for c-IAP2, 5'-CAATGAATTCGAGATCTACCAGTGGGAAGAA-3' and 5'-CAATCTCGAGTCATGAAAGAAATGTACG-3'; for ML-IAP, 5'-GACTGAATTCTTGCCAGGGATGTGGAGGCG-3' and 5'-CAATCTCGAGTTAGGACAGGAAGGTGCGC-3'; and for XIAP, 5'-GACTGAATTCCTGAGATTAGTACTGAAGAG-3' and 5'-TAGCCTCGAGTTAAGACATAAAAATTTTTTGC-3'. The resultant products were subsequently digested with EcoRI and XhoI, and ligated into the pACT2 vector (Clontech).

siRNA oligonucleotides

The following siRNA oligonucleotides were used in gene silencing experiments: for the UbcH5 family, a pool of 5'-CCAAAGATTGCTTTCACAATT-3' and 5'-GGTGGAGTCTTCTTTCTCATT-3' targeting UbcH5a, together with 5'-CAGTAATGGCAGCATTGT-3' and 5'-GATCACAGTGGTCGCCTGC-3' both targeting UbcH5b and UbcH5c; for UbcH13, a pool previously described was used (Zhou et al, 2004); for Rad6b, a pool of 5'-GGAATGCAGTTATATTTGGTT-3', 5'-GAACCGAATCCTAACAGTCTT-3', and 5'-GAGTTTCGGCCATTGTTGATT-3'; for Ube2s, a pool previously described was used (Tedesco et al, 2007); for Ube2Q2, a pool of 5'-GTATGGAAGTTCTCACAAATT-3', 5'-TTATATGACTGGCATGTTATT-3', and 5'-GCCCAACAATCCTATAATTTT-3'; for tsg101, a pool of 5'-CCTCCAGTCTTCTCTCGTCTT-3' and 5'-CCAGTCTTCTCTCGTCCTATT-3'; scramble II (Dharmacon) siRNA was used for a negative control in siRNA transfections.

Real-time quantitative PCR

RNA samples from siRNA treated cells were prepared and real-time PCR analysis was performed as previously described (Dynek et al, 2008). The following sequences were used: for detection of Rad6B, 5'-TTCAAGCGGTTACAAGAGGA-3' (F), 5'-ACTGCATTCCACTGCATGAT-3' (R), and 5'-FAM-ATGGTGCGCCACTGACACCC-TAMRA-3' (probe); for Ube2Q2, 5'-CAACAATTTGCTTCGTCAGC-3' (F), 5'-CTTCTTCTGTTGTCCCATTCTG-3' (R), and 5'-FAM-TGCTAGATCAACCACTACCCACGGG-TAMRA-3'; for *RelB*, 5'-GCCGAATTAACAAGGAAAGC (F), 5'-CCTTGTCGCAGAGCAAGTAG (R), 5'-FAM-CTCCTCGCCACCGGTGCAC-TAMRA (probe), for *IL-8*, 5'-TGCTAGCCAGGATCCACAAGT (F), 5'-TGTGAGGTAAGATGGTGGCTAATACT (R), 5'-FAM-TCCACTGTGCCTTGGTTTCTCCTTTATTCTAAGT-TAMRA (probe), for *MCP-1*, 5'-TCAGCCAGATGCAGTTAACGC (F), 5'-TGATCCTCTTGAGCTCTCCAGC (R), 5'-FAM-CCACTCACCTGCTGCTACTCATTCACCA-TAMRA (probe), and for *RPL19*, 5'-AGCGGATTCTCATGGAACA (F), 5'-CTGGTCAGCCAGGAGCTT (R), 5'-FAM-TCCACAAGCTGAAGGCAGACAAGG-TAMRA (probe).

MS analysis of RIP1 ubiquitination

Gel regions from a Coomassie stained SDS-PAGE gel were excised, destained, dehydrated, and then reswollen on ice for 20 min in 20 ng/μl trypsin, 50mM ammonium bicarbonate/5% acetonitrile. Samples were digested for 16 hr at 37°C. A mixture of isotopically labeled internal standard peptides to Ub (Blankenship et al, 2009; Kirkpatrick et al, 2006), RIPK (IADLGLASFK, and LLGVIIIEGK) and c-IAP1 (AGFYIIGPGDR, and LFPGPSYQNIK) (150 fmol) were added, and the peptides subsequently extracted using 50% acetonitrile/5% formic acid. Samples were dried completely, and dry peptides were resuspended in 4% acetonitrile/5% formic acid/0.01% H₂O₂ at least 30 min before injection via an autosampler onto a NanoAcquity UPLC system (Waters, Dublin, CA). Peptides were separated at 1 μl/min on a 0.1x100 mm BEH-130 C18 column (Waters,

Milford, MA) by a 35 min gradient of 2%-25% solvent B (98% acetonitrile/2% H₂O /0.1% formic acid) in solvent A (98% H₂O /2% acetonitrile/0.1% formic acid). Peptides were eluted directly into an ADVANCE nanospray ionization source (Michrom, Auburn, CA) with a spray voltage of 1.4 kV and analyzed using an LTQ XL-Orbitrap mass spectrometer (ThermoFisher, San Jose, CA). Precursor ions were analyzed in the FTMS at 60,000 resolution, and the top 4 most abundant ions subjected to data dependent MS/MS in the ion trap. Peptides from the sample were quantified from narrow window extracted ion chromatograms relative to their co-eluting internal standards.

Recombinant protein purification

NEMO_{UBD} (G257-S346) and c-IAP1_{BIR3-RING} (M266-S618) constructs were each made with a TEV-cleavable, N-terminal His-tag followed by an Avi-tag sequence (MHHHHHHGENLYFQ/SGLNDIFEAQKIEWHEGS); the latter enabling site-specific biotinylation of the proteins by the BirA biotin ligase (Smith et al, 1998). Specifically, the tagged constructs were co-expressed with BirA in BL21 pLysS cells grown in LB media (plus 50 mM zinc acetate for c-IAP1_{BIR3-RING}). Cultures were grown at 37 °C to an OD600 of 1.0, then moved to 16 °C where they were supplemented with 50 µM biotin, induced with 0.75 mM IPTG and harvested after 18 hours of growth. Cell pellets were flash frozen in liquid nitrogen, then thawed and resuspended in Buffer A [25 mM Tris pH8, 0.3 M NaCl, 10 mM imidazole, 0.5mM TCEP] with the following additives: 50 µg/mL lysozyme, 10 µg/mL Dnase and cOmplete, EDTA-free protease inhibitor cocktail tablets (Roche).

Cells were lysed by successive passages through a microfluidizer and centrifuged to pellet cell debris (this and all subsequent purification steps conducted at 4 °C). The supernatant was added to nickel agarose beads pre-equilibrated with Buffer A and incubated with agitation for 30 minutes prior to loading onto EconoPack disposable columns (BioRad). The packed columns were washed with Buffer B [25 mM Tris pH8, 0.3 M NaCl, 10 mM imidazole, 0.5mM TCEP] and protein eluted by increasing the imidazole concentration to 300mM. The eluted material was concentrated and buffer exchanged with Gel Filtration (GF) Buffer [25 mM Tris pH8, 0.3 M NaCl, 0.5mM TCEP] in 10 kDa MWCO Ultrafree concentrators (Millipore) until < 1 mM imidazole remained. The concentrated stock was treated with ~1 mg TEV protease overnight, passed over a 1mL Ni-NTA column (BioRad) pre-equilibrated with GF Buffer and the TEV-cleaved material collected in the flow through was further purified by size exclusion chromatography. Monomeric c-IAP1_{BIR3-RING} and dimeric NEMO_{UBD} each eluted as a single peak from a Superdex 75 column (GE Lifescience) and were stored at 4 °C in GF buffer.

The linear Ub dimer gene (M1-G152) was synthesized by GenScript and sub-cloned into the same pET15b expression vector as the Ub monomer construct (M1-G76). Both Ub monomer and dimer constructs, which each contain an N-terminal His-tag and thrombin cleavage site (MGSSHHHHHSSGLVPR/GSH), were expressed and purified as previously described (Matsumoto et al, 2010; Newton et al, 2008). K11, K48 and K63 Ub dimers were prepared from Ub monomer stocks using a modified version of the enzymatic protocol described (Raasi & Pickart, 2005) and purified on a MonoS column with a NaCl gradient and ammonium acetate pH 4.5.

Coding region for Ubch5a was cloned into pGEX6p1, creating construct with N-terminal, PreScission Protease-cleavable GST-tag. Protein was expressed in E. coli BL21-CodonPlus(DE3)-RIL cells. Cells were grown at 37 °C in LB media to an OD₆₀₀ of 0.6-0.7, induced with 0.5 mM IPTG, transferred to 16 °C and expressed for 16 hrs. For purification, cells were resuspended in lysis buffer [20mM Tris, 150mM NaCl, 1 mM TCEP, pH 7.8] supplemented with protease inhibitor cocktail tablets (Roche), lysed by passing through microfluidizer and centrifuged. Protein was captured by glutathione sepharose 4B beads, which were thoroughly washed and resuspended in cleavage buffer [20 mM Tris, 150 mM NaCl, 1 mM TCEP, pH 7.8]. On-column removal of GST-tag by PreScission Protease conducted at 4 °C for 16 hrs, after which the flow-through was collected and applied to a S75 gel filtration column equilibrated with [20 mM Tris, 150 mM NaCl, 1 mM TCEP, pH 7.8] buffer. Monomeric Ubch5a fractions were pooled, concentrated and stored at -20 °C.

Supplemental Figure Legends

Supplemental Figure 1. IAP RING constructs interactions with E2 ubiquitin-conjugating enzymes by yeast two-hybrid analysis. Interactions observed for each directed yeast two-hybrid screen with IAP RING domain DNA-binding fusion bait constructs (c-IAP1 RING, c-IAP2 RING, ML-IAP RING, XIAP RING) and all E2 activation domain fusion prey constructs tested. Interactions were scored according to growth on selective medium; a + indicates growth present; a – indicates growth absent.

Supplemental Figure 2. Positive and Negative controls used in IAP-RING-E2 yeast two-hybrid screen. The BRCA1 RING-BARD1 RING fusion bait construct, BD126FBC109, was cotransformed with Ubch5b, or Ubch5c prey, constructs as a positive controls for the screen. The ligase inactive BRCA1 RING mutation I26A containing bait construct, BD126FBC109 I26A, was cotransformed with Ubch5b, or Ubch5c prey, constructs as a negative controls for the screen. The TRAF6 RING bait construct was cotransformed with the Ubch13 prey construct, as a positive control for Ubch13 interactions in the screen. The TRAF2 RING bait construct served as a negative control for Ubch13, Ubch5b, and Ubch5c interactions. Interactions were scored according to growth on selective medium; a + indicates growth present; a – indicates growth absent.

Supplemental Figure 3. Analyses of interactions E2 enzymes with IAP-RING domains. (A) The indicated E2 prey constructs were cotransformed with the WT c-IAP1 RING construct, or the IAP RING E2 binding interface mutant (c-IAP1 RING V573A), or the IAP RING dimerization mutant (c-IAP1 RING F616A) bait constructs. (B) The indicated E2 prey constructs were cotransformed with the WT ML-IAP RING construct, or the ML-IAP RING E2 binding interface mutants (ML-IAP RING V254A), or the ML-IAP RING dimerization mutant (ML-IAP RING F296A) bait constructs. (C) The Ubch9 prey construct was cotransformed with WT IAP RING constructs, IAP RING E2 binding interface mutants (c-IAP1 RING V573A, c-IAP2 RING V559A, ML-IAP RING V254A, XIAP RING I452A), and IAP RING dimerization mutants (c-IAP1 RING F616A, c-IAP2 RING F602A, ML-IAP RING F296A, XIAP RING 495A) bait

constructs. Interactions were scored according to growth on selective medium; a + indicates growth present; a – indicates growth absent.

Supplemental Figure 4. (A) Quantification of ubiquitin linkages from reactions shown in Figure 2 using isotopically labeled internal standards. Data for the three primary linkages are shown relative to the sum of all linkages. (B) During the analysis, data were collected for two peptides derived from c-IAP1 (LFPGPSYQNIK, AGFYIIGPGDR). Signal from c-IAP1 peptides was detected in all gel regions, and was more abundant in regions where significant levels of ubiquitin were detected. The correlation between c-IAP1 and ubiquitin in the gel regions where Ub-c-IAP1 would be expected to migrate indicates that c-IAP1 is the major ubiquitin substrate being detected.

Supplemental Figure 5. Expression and stability of IAP proteins. (A) HKB11-CD40 cells were treated with cross-linked anti-CD40 antibody at a concentration of 0.5 µg/ml for 0, 5, or 30 minutes. Lysates were collected and subjected to Western blot analysis using antibodies specific for c-IAP1, XIAP, c-IAP2, ML-IAP, and actin, as a loading control. Lysates from HKB11-CD40 cells ectopically expressing ML-IAP and c-IAP2 in were used as positive controls for detection of these IAP proteins. (B) siRNA knockdown of the UbcH5 family increases the stability of c-IAP1 following IAP antagonist treatment. Hek293T cells were transfected with control siRNA, or siRNA targeting the UbcH5 family (UbcH5a, UbcH5b, UbcH5c isoforms). 48 hours later cells were treated with, or without, 5µM IAP antagonist (MV1) for 10 minutes. Lysates were collected and subject to western blot analysis using antibodies for detection of c-IAP1, UbcH5 (the antibody recognizes all three isoforms), and actin, as a loading control.

Supplemental Figure 6. Knockdown of UbcH5 family inhibits gene induction by TNFα. HT1080 or HeLa S cells were treated with TNFα for 4 hours, and RNA samples from treated and untreated cells were analyzed by quantitative real-time PCR analysis. All values were normalized to an *RPL19* RNA internal control. Columns represent mean from triplicate experiments and bars standard deviation.

Supplemental Figure 7. c-IAP1 and UbcH5 regulate NIK stability. (A) NIK protein stability in the presence of the c-IAP1 proteins. HEK293T cells were transfected with myc-NIK1 plus FLAG-c-IAP1, or FLAG-c-IAP1 F616A (FA) or FLAG-c-IAP1 V573A/D576A (VD/AA) mutants, or FLAG-vector. The following day, lysates were collected and analyzed by Western blotting. (B) NIK protein stability in the presence of the c-IAP1 and siRNA-resistant UbcH5 proteins. 293T cells were transfected with control siRNA, or siRNA targeting the UbcH5 family. 24 hours later, cells were transfected with myc-NIK1 plus siRNA-resistant UbcH5b (UbcHb/rs) and FLAG-c-IAP1, or FLAG-vector. The following day, lysates were collected and analyzed by Western blotting.

Supplemental Figure 8. c-IAP1 promotes K11-linked polyubiquitination of RIP1. (A) RIP1 ubiquitination by E2-binding or dimerization deficient c-IAP1 mutants. HEK293T cells were transfected with myc-RIP1, HA-tagged ubiquitin, and FLAG-c-IAP1, or FLAG-c-IAP1 F616A (FA), or FLAG-c-IAP1 V573A/D576A (VD/AA), or FLAG-vector for 24 hours. Cells were pre-treated with MG132 (20 µM) for 1 hour,

lysates were boiled in NP40 lysis buffer containing 1% SDS for 10 minutes, diluted 10-fold and immunoprecipitated using anti-myc or anti-Flag beads. Flag c-IAP1 proteins and myc-RIP1 were detected in immunoprecipitated material and input lysates using anti-myc and anti-Flag antibodies, and anti-HA antibody to detect ubiquitinated species. (B) RIP1 ubiquitination requires catalytically active c-IAP1. c-IAP1 knockout MEFs were transiently transfected with HA-Ub and vector, or Flag-c-IAP1, or Flag-c-IAP1 F616A (FA) for 24 hours. Cells were pre-treated with MG132 (20 μ M) for 1 hour, lysates were denatured in NP40 lysis buffer containing 6 M urea for 20 minutes, diluted 12-fold and immunoprecipitated using anti-K11 antibodies. Ubiquitinated RIP1 was detected in immunoprecipitated material and input lysates using anti-RIP1 antibodies. (C, D and E) c-IAP1 and the UbcH5 family of E2 enzymes promote assembly of K11-linked polyubiquitin chains on c-IAP1 and RIP1. Recombinant c-IAP1 was incubated for 45 minutes in a ubiquitination reaction alone (C) or with RIP1 with UbcH5a, b, or c and wild type ubiquitin, or with UbcH5a and K11R (11R), K48R (48R), K63R (63R) ubiquitin proteins (D). Western blotting was performed with anti-ubiquitin (C and D) and anti-RIP1 (D) antibodies to detect ubiquitinated c-IAP1 and RIP1. (E) Recombinant RIP1 was incubated with c-IAP1 and UbcH5a or Ube2S in a two-step reaction as described in Figure 2 in the presence of wild type or K11R ubiquitin (11R). RIP1 modifications were determined by Western blot analysis with anti-RIP1 and anti-ubiquitin antibodies.

Supplemental Figure 9. c-IAP2 promotes K11-linked polyubiquitination of RIP1.

Recombinant c-IAP2 was incubated for 45 minutes in a ubiquitination reaction with UbcH5a, b, or c and wild type ubiquitin (A), or with UbcH5b and K11R (11R), K48R (48R), K63R (63R) ubiquitin proteins, and reactions analyzed by Western blot with anti-ubiquitin antibodies (B). (C) c-IAP2 and the UbcH5b promote assembly of K11-linked polyubiquitin chains on RIP1. Recombinant RIP1 was incubated for 45 minutes in a ubiquitination reaction in the absence or the presence of recombinant c-IAP2, UbcH5b and wild-type or K11-only (11) ubiquitin proteins. RIP1 modifications were detected by Western blot with anti-RIP1 and anti-ubiquitin antibodies.

Supplemental Figure 10. Characterization of c-IAP1 mediated ubiquitin linkages on RIP1.

(A) Recombinant RIP1 was incubated for 45 minutes in ubiquitination reactions in the absence or presence of recombinant c-IAP1, UbcH5a and wild type ubiquitin. Following ubiquitination reactions, samples were incubated in 6M Urea at room temperature for 30 minutes with rocking, diluted 15 times and immunoprecipitated using anti-RIP1 antibodies. RIP1 and c-IAP1 modifications were determined with anti-RIP1, anti-ubiquitin and anti-c-IAP1 antibodies. (B) List of peptides used for quantitative analysis of c-IAP1 and RIP1.

Supplemental Figure 11. TNF α stimulates K11-linked polyubiquitination of RIP1.

(A) HT29 cells were treated with or without 100 ng/ml of TNF α for 10 minutes. Cells were harvested, lysed and protein samples denatured in 6M urea. Immunoprecipitations were performed using the indicated antibodies in 4M urea overnight, followed by washes in lysis buffer, and Western blot analysis with anti-RIP1 antibody. (B) Stability of K11-linked polyubiquitinated RIP1 in response to TNF α . HeLa S3 cells were pretreated with or without 20 μ M MG132 for 1 hour and subsequently treated with or without 100 ng/ml

of TNF α for 10 minutes. Cells were harvested, lysed and protein samples were denatured in 6M urea. Immunoprecipitations and western blotting were performed as in (A). (C) Stability of TNFR1-bound K11-linked polyubiquitinated RIP1 in response to TNF α . HeLa S3 cells were pretreated with or without 20 μ M MG132 for 30 minutes, and then incubated with or without 100 ng/ml of TNF α for 5 or 20 minutes. Lysates were collected and subjected to serial immunoprecipitations, first using anti-TNFR1 antibodies, and then after eluting under denaturing (6M urea) conditions secondary immunoprecipitations were performed using a K11 linkage-specific anti-ubiquitin antibody. Input lysates, left panel, were analyzed by western blot with anti-RIP1, anti-I κ B α , and anti-c-IAP1 antibodies. Eluates from serial immunoprecipitations, right panel, were detected using anti-RIP1 antibody.

Supplemental Figure 12. Association of endogenous NEMO and RIP1 with K11-linked ubiquitin chains. HeLa S3 cells were pretreated with 20 μ M MG132 for 30 minutes and then treated with or without 100 ng/ml of TNF α for 10 minutes. Cells were harvested, lysed and protein samples were immunoprecipitated using control, K11- or K63-specific antibodies. Western blotting of cellular lysates and immunoprecipitates was performed with the indicated antibodies.

Supplemental Table I. Taqman Analysis of gene silencing in Figure 3A untreated samples.

| siRNA | Percent mRNA levels | |
|--------|---------------------|--------|
| | Rad6B | Ube2Q2 |
| ctrl | 100 | 100 |
| Rad6B | 16 | n.t. |
| Ube2Q2 | n.t. | 6 |

Supplemental Table II. Taqman Analysis of gene silencing in Figure 3B.

| DNA: | siRNA: | Percent mRNA levels | |
|--------------|--------|---------------------|----------------|
| | | Rad6B | Ube2Q2 |
| NIK + Vector | ctrl | 100* | 100* |
| NIK + Vector | Rad6B | 27* | n.t. |
| NIK + Vector | Ube2Q2 | n.t. | 34* |
| NIK + c-IAP1 | ctrl | 100 \ddagger | 100 \ddagger |
| NIK + c-IAP1 | Rad6B | 11 \ddagger | n.t. |
| NIK + c-IAP1 | Ube2Q2 | n.t. | 20 \ddagger |
| NIK + c-IAP2 | ctrl | 100 \S | 100 \S |
| NIK + c-IAP2 | Rad6B | 14 \S | n.t. |
| NIK + c-IAP2 | Ube2Q2 | n.t. | 31 \S |

* samples calibrated to NIK + vector + ctrl siRNA

\ddagger samples calibrated to NIK + c-IAP1 + ctrl siRNA

\S samples calibrated to NIK + c-IAP2 + ctrl siRNA

References

- Blankenship JW, Varfolomeev E, Goncharov T, Fedorova AV, Kirkpatrick DS, Izrael-Tomasevic A, Phu L, Arnott D, Aghajan M, Zobel K, Bazan JF, Fairbrother WJ, Deshayes K, Vucic D (2009) Ubiquitin binding modulates IAP antagonist-stimulated proteasomal degradation of c-IAP1 and c-IAP2. *Biochem J* **417**: 149-160
- Dynek JN, Chan SM, Liu J, Zha J, Fairbrother WJ, Vucic D (2008) Microphthalmia-associated transcription factor is a critical transcriptional regulator of melanoma inhibitor of apoptosis in melanomas. *Cancer Res* **68**: 3124-3132
- Kirkpatrick DS, Hathaway NA, Hanna J, Elsasser S, Rush J, Finley D, King RW, Gygi SP (2006) Quantitative analysis of in vitro ubiquitinated cyclin B1 reveals complex chain topology. *Nat Cell Biol* **8**: 700-710
- Matsumoto ML, Wickliffe KE, Dong KC, Yu C, Bosanac I, Bustos D, Phu L, Kirkpatrick DS, Hymowitz SG, Rape M, Kelley RF, Dixit VM (2010a) K11-linked polyubiquitination in cell cycle control revealed by a K11 linkage-specific antibody. *Mol Cell* **39**: 477-484
- Newton K, Matsumoto ML, Wertz IE, Kirkpatrick DS, Lill JR, Tan J, Dugger D, Gordon N, Sidhu SS, Fellouse FA, Komuves L, French DM, Ferrando RE, Lam C, Compaan D, Yu C, Bosanac I, Hymowitz SG, Kelley RF, Dixit VM (2008) Ubiquitin chain editing revealed by polyubiquitin linkage-specific antibodies. *Cell* **134**: 668-678
- Raasi S, Pickart CM (2005) Ubiquitin chain synthesis. *Methods Mol Biol* **301**: 47-55
- Smith PA, Tripp BC, DiBlasio-Smith EA, Lu Z, LaVallie ER, McCoy JM (1998) A plasmid expression system for quantitative in vivo biotinylation of thioredoxin fusion proteins in *Escherichia coli*. *Nucleic Acids Res* **26**: 1414-1420
- Tedesco D, Zhang J, Trinh L, Lalehzadeh G, Meisner R, Yamaguchi KD, Ruderman DL, Dinter H, Zajchowski DA (2007) The ubiquitin-conjugating enzyme E2-EPF is overexpressed in primary breast cancer and modulates sensitivity to topoisomerase II inhibition. *Neoplasia (New York, NY)* **9**: 601-613
- Zhou H, Wertz I, O'Rourke K, Ultsch M, Seshagiri S, Eby M, Xiao W, Dixit VM (2004) Bcl10 activates the NF-kappaB pathway through ubiquitination of NEMO. *Nature* **427**: 167-171

| Prey \ Bait | c-IAP1 RING | c-IAP2 RING | ML-IAP RING | XIAP RING |
|-------------|-------------|-------------|-------------|-----------|
| FT1 | – | – | – | – |
| tsg101 | + | – | – | – |
| Rad6B | + | – | – | – |
| UbcH10 | – | – | – | – |
| UbcH5a | + | + | + | + |
| UbcH5b | + | + | + | + |
| UbcH5c | + | + | + | + |
| UbcH6 | – | – | + | + |
| Ube2E2 | – | – | – | – |
| UbcM2 | – | – | – | – |
| Ube2F | – | – | – | – |
| Ube2G | – | – | – | – |
| Ube2H | – | – | – | – |
| Ubc9 | – | + | + | + |
| Ube2K | – | – | – | – |
| UbcH8 | – | – | – | – |
| UbcH7 | – | – | – | – |
| UbcH12 | – | – | – | – |
| UbcH13 | – | – | – | – |
| Ube2Q2 | + | + | – | – |
| CDC34 | – | – | – | – |
| Ube2S | + | – | – | – |
| Ube2T | – | – | – | – |
| Ube2U | – | – | – | – |
| Ube2V1 | – | – | – | – |
| Mms2 | – | – | – | – |
| Ube2V3 | – | – | – | – |
| Ube2W | – | – | – | + |
| Ube2Z | – | – | – | – |
| Uev1b | – | – | – | – |
| pACT2 | – | – | – | – |

Dynek et al, Supplemental Figure 2

| Bait \ Prey | UbcH5b | UbcH5c | UbcH13 |
|------------------|--------|--------|--------|
| BD126FBC109 | + | + | n.t. |
| BD126FBC109 I26A | – | – | n.t. |
| TRAF2 RING | – | – | – |
| TRAF6 RING | n.t. | n.t. | + |

Dynek et al, Supplemental Figure 3

S3A

| Bait \ Prey | c-IAP1 | c-IAP1 V573A | c-IAP1 F616A |
|--------------|--------|--------------|--------------|
| Rad6B | + | – | – |
| Ube2Q2 | + | – | – |
| Ube2S | + | – | – |
| c-IAP1 pACT2 | + | + | – |

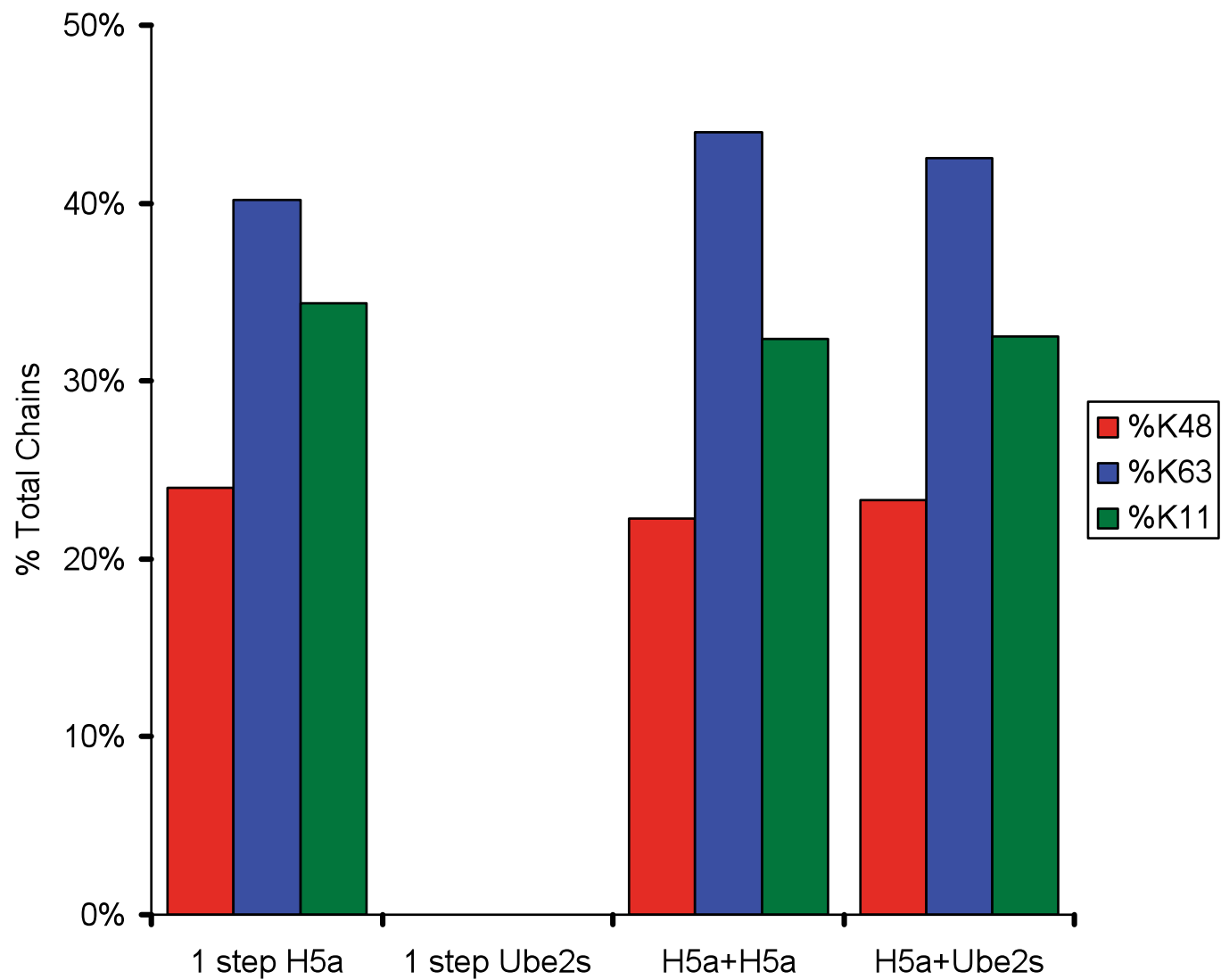
S3C

| Bait \ Prey | Ubc9 |
|-------------------|------|
| c-IAP1 RING | – |
| c-IAP1 RING V573A | – |
| c-IAP1 RING F616A | – |
| c-IAP2 RING | + |
| c-IAP2 RING V559A | + |
| c-IAP2 RING F602A | + |
| ML-IAP RING | + |
| ML-IAP RING V254A | + |
| ML-IAP RING F296A | + |
| XIAP RING | + |
| XIAP RING 452A | + |
| XIAP RING F495A | + |

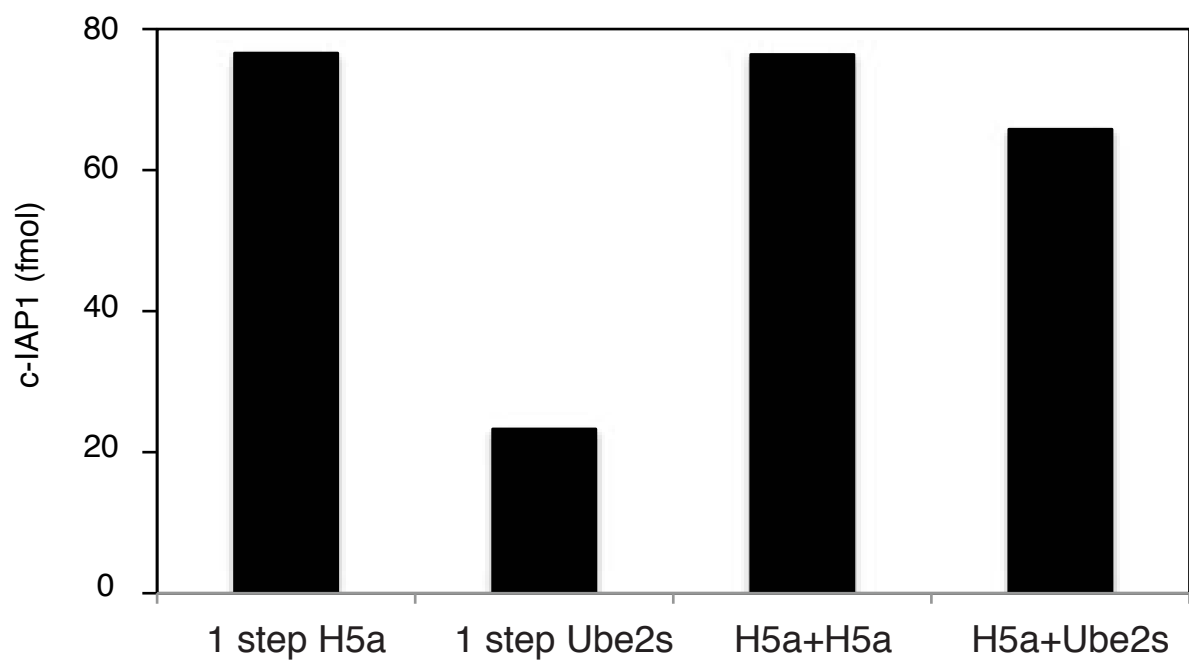
S3B

| Bait \ Prey | ML-IAP | ML-IAP V254A | ML-IAP F296A |
|--------------|--------|--------------|--------------|
| UbcH5a | + | – | – |
| UbcH5b | + | – | – |
| UbcH5c | + | – | – |
| UbcH6 | + | – | – |
| c-IAP1 pACT2 | + | + | – |

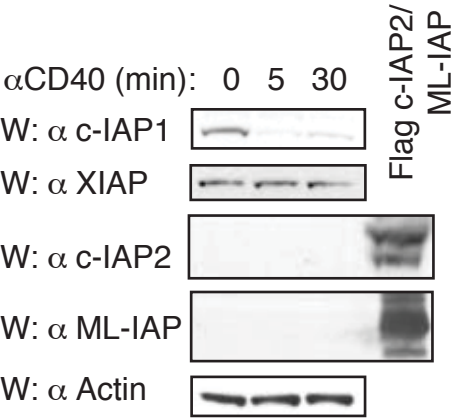
S4A



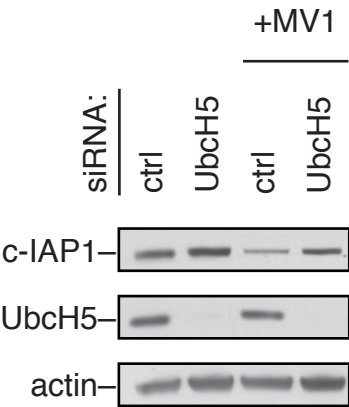
S4B



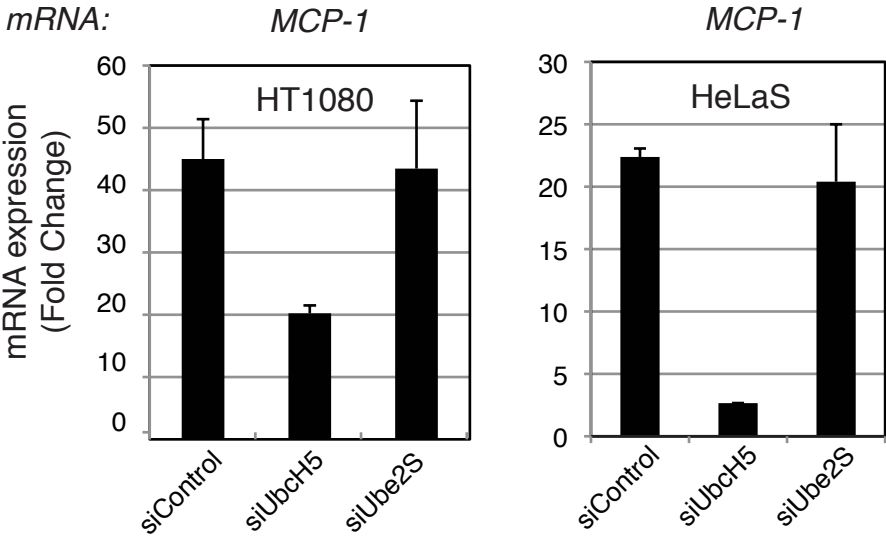
S5A



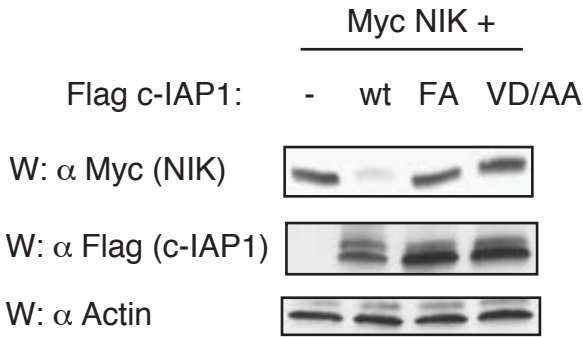
S5B



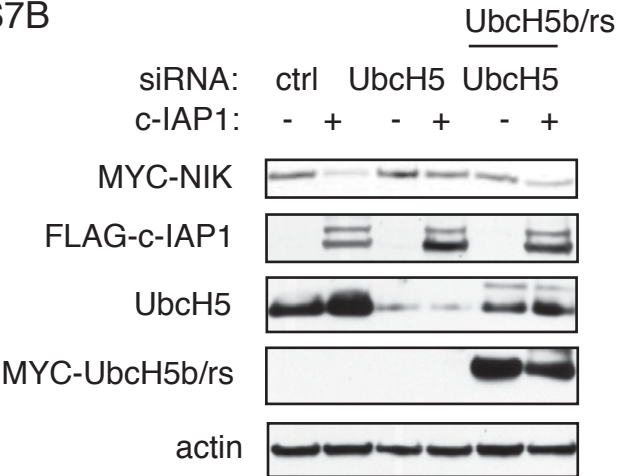
S6



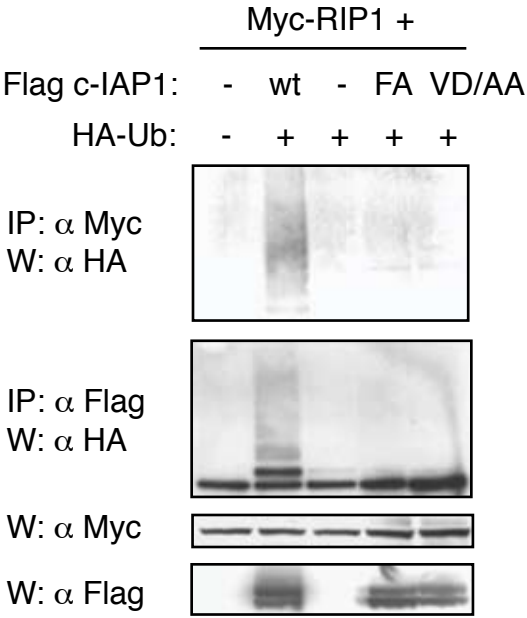
S7A



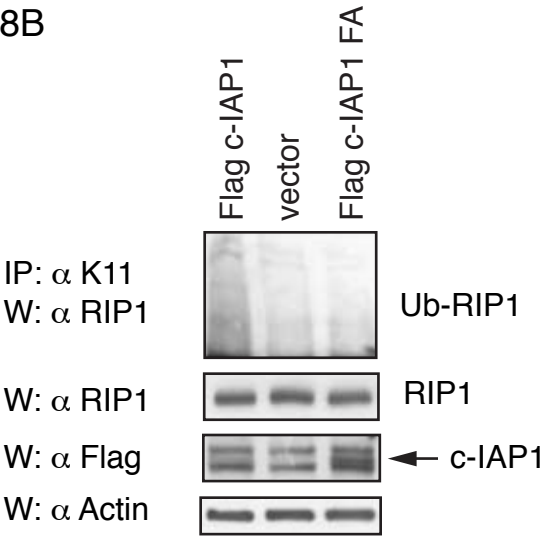
S7B



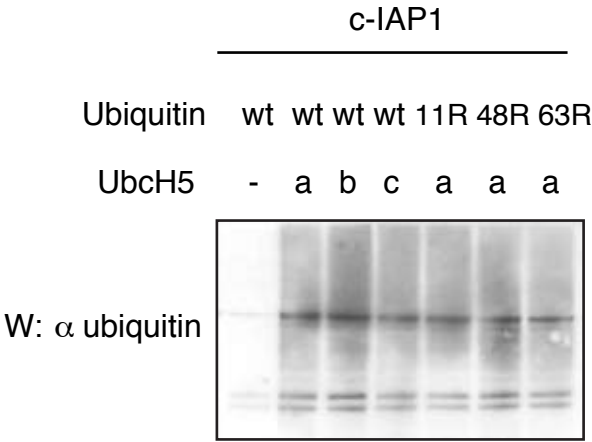
S8A



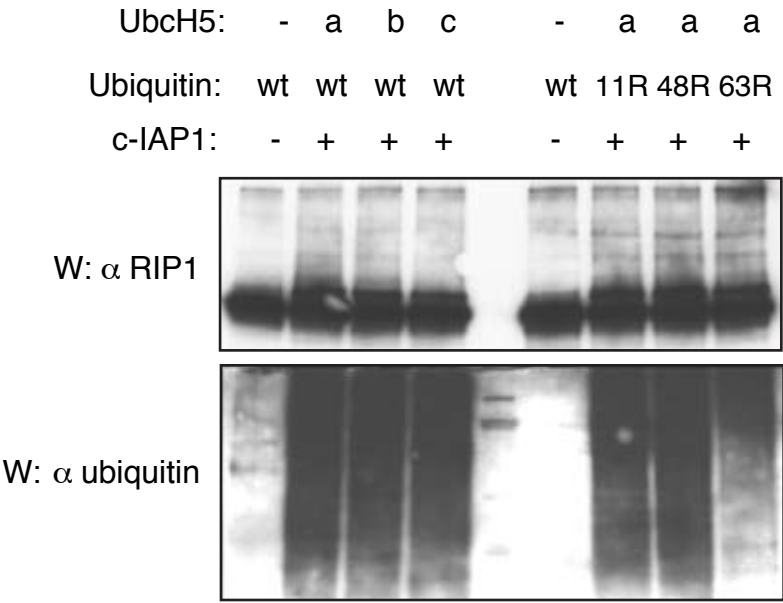
S8B



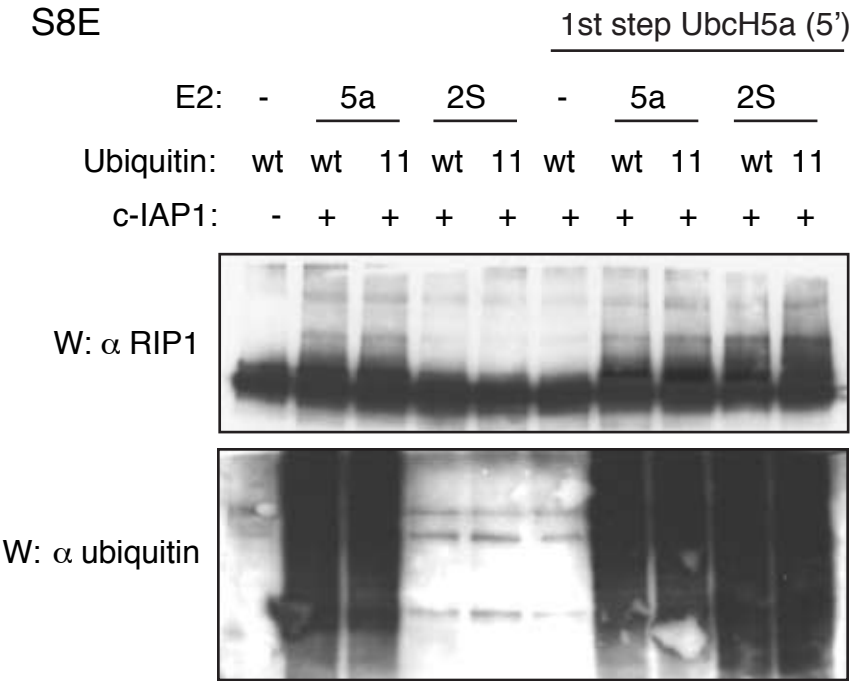
S8C



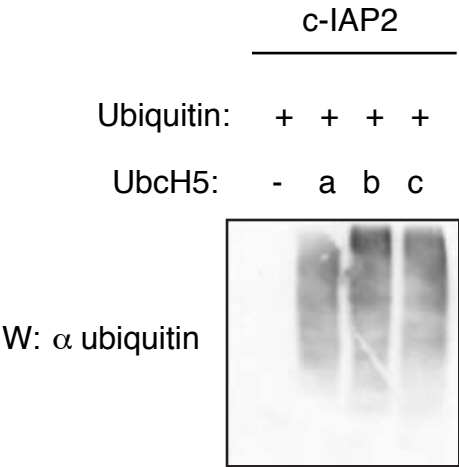
S8D



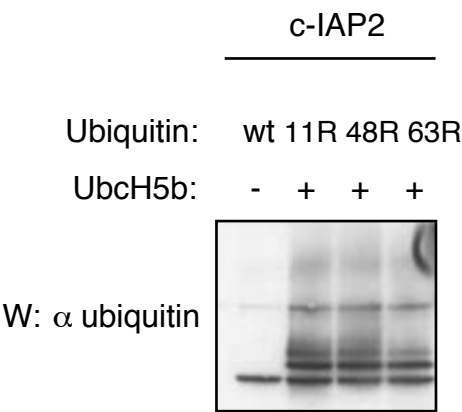
S8E



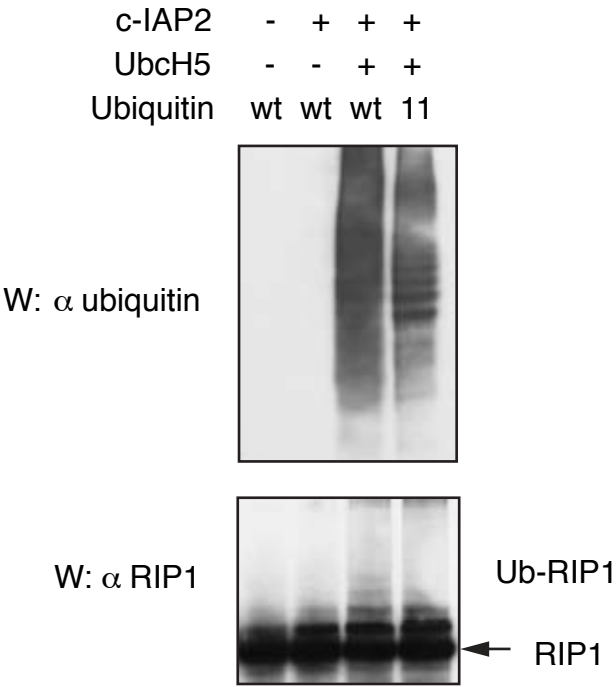
S9A



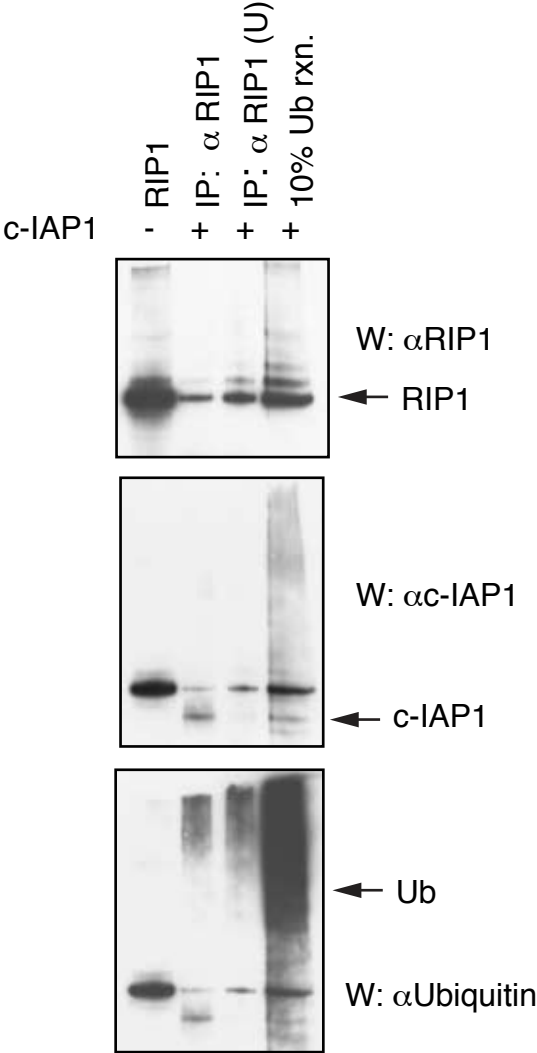
S9B



S9C



SF10A

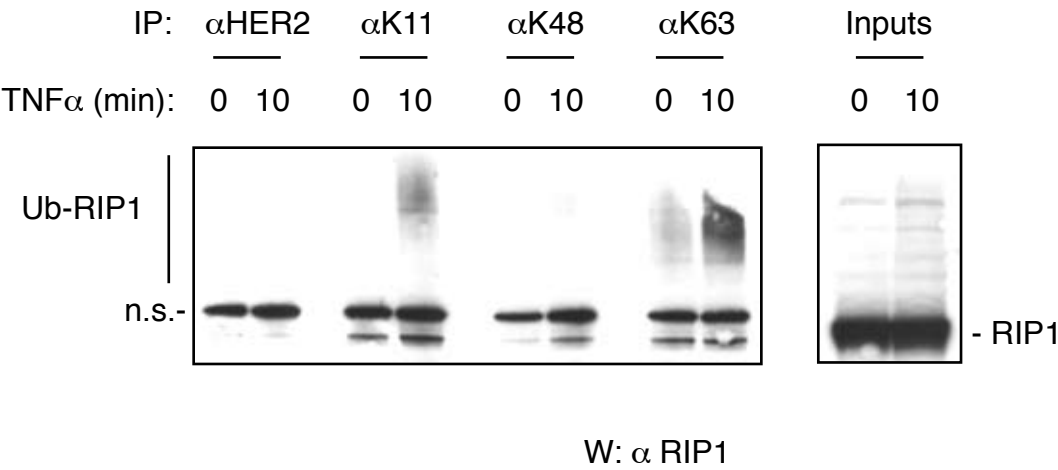


SF10B

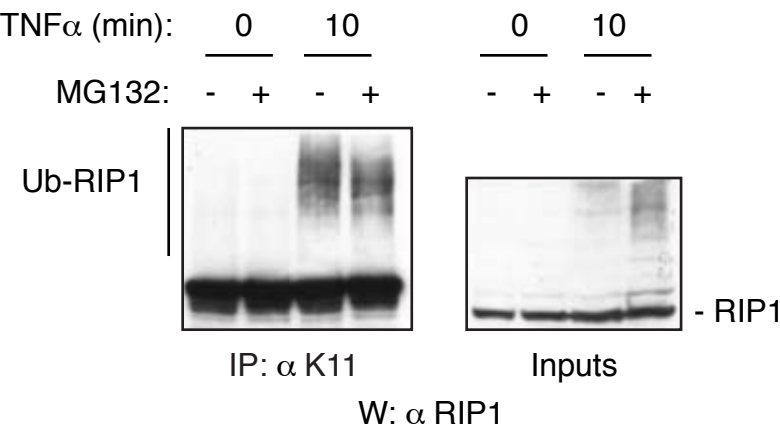
| c-IAP1 peptide | m/z (Heavy / Light) |
|--------------------------|------------------------|
| AGFY ^P IGDR | 611.3002 / 608.2933 |
| LFPG ^P SYQNIK | 635.3471 / 632.3402 |

| RIP1 peptide | m/z (Heavy / Light) |
|-------------------------|------------------------|
| IADLG ^L ASFK | 521.3063 / 517.7977 |
| LLG ^V IIEEGK | 538.8333 / 535.8264 |

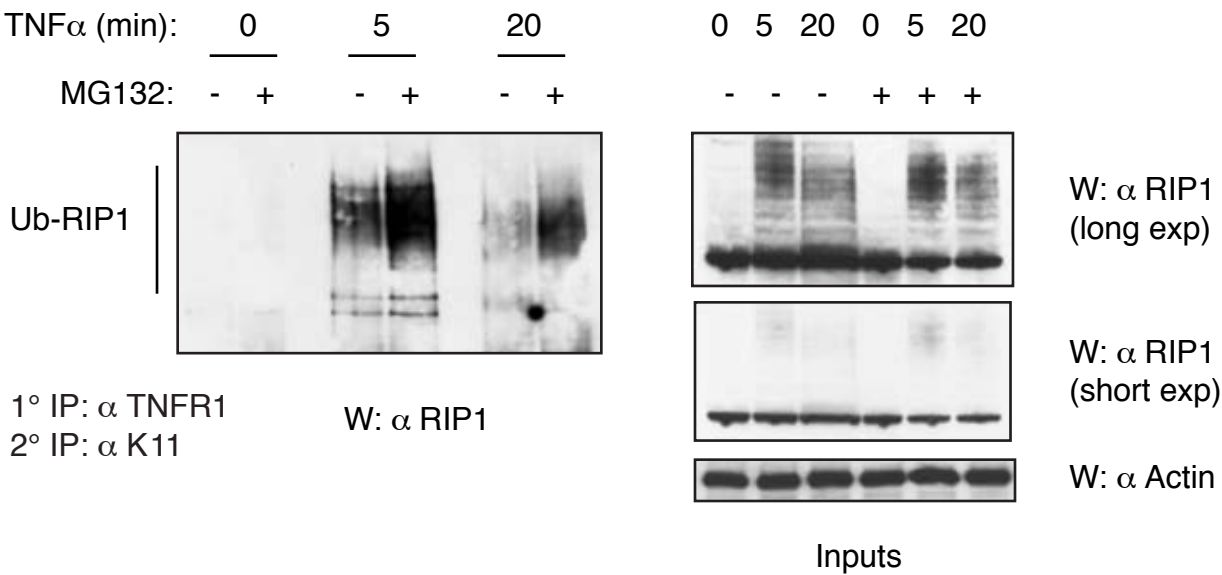
SF11A



SF11B



SF11C



SF12

